

1 **Title Page**

2 Effects of land use/land cover and climate changes on surface runoff in a  
3 semi-humid and semi-arid transition zone in Northwest China

4 Jing Yin <sup>1</sup>, Fan He <sup>2</sup>, YuJiu Xiong <sup>3,4,\*</sup>, GuoYu Qiu <sup>5,\*</sup>

5 <sup>1</sup> Research Center for Sustainable Hydropower Development, China Institute of  
6 Water Resources and Hydropower Research, Beijing 100038, China.

7 <sup>2</sup> State Key Laboratory of Simulation and Regulation of Water Cycle in River  
8 Basin, China Institute of Water Resources and Hydropower Research, Beijing 100038,  
9 China.

10 <sup>3</sup> Department of Water Resource and Environments, School of Geography and  
11 Planning, Sun Yat-Sen University, Guangzhou 510275, Guangdong, China.

12 <sup>4</sup> Department of Land, Air and Water Resources, University of California at Davis.

13 <sup>5</sup> Shenzhen Engineering Laboratory for Water Desalinization with Renewable  
14 Energy, School of Environment and Energy, Peking University, Shenzhen 518055,  
15 Guangdong, China.

16

---

First author Email address: [yingjing@iwhr.com](mailto:yingjing@iwhr.com)

\* Corresponding author: YuJiu Xiong, Email address: [xiongyuj@mail.sysu.edu.cn](mailto:xiongyuj@mail.sysu.edu.cn).  
Tel./Fax: +86 20 84114575.

Co-corresponding author: GuoYu Qiu, Email address: [qiugy@pkusz.edu.cn](mailto:qiugy@pkusz.edu.cn). Tel./Fax:  
+86 755 26033309.

17 **Abstract**

18 Water resources, which are considerably affected by land use/land cover (LULC)  
19 and climate changes, are a key limiting factor in highly vulnerable ecosystems in arid  
20 and semi-arid regions. The impacts of LULC and climate changes on water resources  
21 must be assessed in these areas. However, conflicting results regarding the effects of  
22 LULC and climate changes on runoff have been reported in relatively large basins, such  
23 as the Jinghe River Basin (JRB), which is a typical catchment ( $> 45000 \text{ km}^2$ ) located in  
24 a semi-humid and arid transition zone on the central Loess Plateau, Northwest China. In  
25 this study, we focused on quantifying both the combined and isolated impacts of LULC  
26 and climate changes on surface runoff. We hypothesized that under climatic warming  
27 and drying conditions, LULC changes, which are primarily caused by intensive human  
28 activities such as the Grain for Green Program, will considerably alter runoff in the JRB.  
29 The Soil and Water Assessment Tool (SWAT) was adopted to perform simulations. The  
30 simulated results indicated that although runoff increased very little between the 1970s  
31 and the 2000s due to the combined effects of LULC and climate changes, LULC and  
32 climate changes affected surface runoff differently in each decade, e.g., runoff increased  
33 with increased precipitation between the 1970s and the 1980s (precipitation contributed  
34 to 88% of the runoff increase). Thereafter, runoff decreased and was increasingly  
35 influenced by LULC changes, which contributed to 44% of the runoff changes between  
36 the 1980s and 1990s and 71% of the runoff changes between the 1990s and 2000s. Our  
37 findings revealed that large-scale LULC under the Grain for Green Program has had an  
38 important effect on the hydrological cycle since the late 1990s. Additionally, the

39 conflicting findings regarding the effects of LULC and climate changes on runoff in  
40 relatively large basins are likely caused by uncertainties in hydrological simulations.

41 **Keywords:** SWAT; climate change; land use/land cover; streamflow; Jinghe River  
42 Basin.

43

## 44 **1 Introduction**

45 Both climate and land use/land cover (LULC) changes are key factors that can  
46 modify flow regimes and water availability (Oki and Kanae, 2006; Piao et al., 2007;  
47 Sherwood and Fu, 2014; Wang et al., 2014a). Since the 20th century, climate variability  
48 is believed to have led to changes in global precipitation patterns (IPCC 2007), thereby  
49 changing the global water cycle and resulting in the temporal and spatial redistribution  
50 of water resources (Milly et al., 2005; Murray et al., 2012). LULC changes are primarily  
51 caused by human activities (Foley et al., 2005; Liu and Li, 2008) and affect the  
52 partitioning of water among various hydrological pathways, including interception,  
53 evapotranspiration, infiltration, and runoff (Sterling et al., 2012). The influences of  
54 climate and LULC changes on hydrological processes and water resources **will likely**  
55 **continue to increase**, especially in arid and semi-arid regions characterized as vulnerable  
56 (Fu, 2003; Vorosmarty et al., 2010).

57 The impacts of LULC and climate changes on runoff can generally be identified by  
58 using hydrological models (Praskievicz and Chang, 2009). These models provide  
59 valuable frameworks for investigating the changes among various hydrological  
60 pathways that are caused by climate and human activities (Leavesley, 1994; Jiang et al.,  
61 2007; Wang et al., 2010). Distributed hydrological models, which use input parameters  
62 that directly represent land surface characteristics, have been applied to assess the  
63 impacts of LULC and climate changes on runoff in water resource management areas  
64 (Yang et al., 2008; Yang et al., 2014; Chen et al., 2015). **The Soil and Water Assessment**  
65 **Tool (SWAT), a robust, interdisciplinary, and distributed river basin model, is**

66 commonly used to assess the effects of management practices and land disturbances on  
67 water quantity and quality (Gassman et al., 2007). The hydrological responses to LULC  
68 and climate changes are often investigated through scenario simulations using the  
69 SWAT model.

70 Although substantial progress has been made in assessing the impacts of LULC  
71 and climate changes on water resources (Krysanova and Arnold, 2008; Vigerstol and  
72 Aukema, 2011; Krysanova and White, 2015), most studies have focused on individual  
73 factors (i.e., either LULC or climate); thus, the combined effects of LULC and climate  
74 changes are not well understood because their contributions are difficult to separate and  
75 vary regionally (Fu et al., 2007; D'Agostino et al., 2010; Wang et al., 2014a). For  
76 example, some studies have suggested that surface runoff is affected more by climate  
77 change (increased precipitation) than by LULC changes (Guo et al., 2008; Fan and  
78 Shibata, 2015), and other studies have found that urbanization contributes more to  
79 increased runoff than precipitation (Olivera and Defee, 2007). According to Krysanova  
80 and White (2015), less than 30 papers were published between 2005 and 2014 on topics  
81 related to the combined effects of LULC and climate changes and the SWAT model,  
82 whereas 210 and 109 papers presented studies of climate and LULC changes,  
83 respectively. However, water resource management requires an in-depth understanding  
84 of the isolated and integrated effects of LULC and climate changes on runoff (Chawla  
85 and Mujumdar, 2015).

86 Notable evidence of drying trends exists in semi-arid and semi-humid regions (Ma  
87 and Fu, 2006; Li et al. 2007; Li et al. 2010; Li et al. 2011). These regions have

88 experienced serious water shortages in addition to intensive human activity and climate  
89 change (Wang and Cheng, 2000; Ma and Fu, 2003). In this case, the effects of LULC  
90 and climate changes on runoff are considerably more sensitive, and a dry climate can  
91 result in serious environmental degradation and water crises (Ma et al., 2008; Jiang et  
92 al., 2011; Leng et al. 2015). The Jinghe River Basin (JRB), which is located on the  
93 central Loess Plateau, is a typical catchment located in a semi-humid and semi-arid  
94 transition zone in Northwest China. The agricultural activities in this basin play an  
95 important role in Northwest China (Zhao et al., 2014). However, the relative importance  
96 of agriculture in the basin has caused ecological problems associated with social  
97 development. For example, local water resources cannot maintain the rapid  
98 socio-economic growth in the region (Wei et al., 2012), and the river system has  
99 become unhealthy (Wu et al., 2014). Water and environmental management in the  
100 region requires improved knowledge of the hydrological impacts of LULC and climate  
101 changes. The effects of LULC and climate changes on the water cycle and water  
102 resources must be assessed in these critical regions (Zhang et al., 2008; Li et al., 2009;  
103 Qiu et al., 2011; Qiu et al., 2012; Peng et al., 2013).

104 Because the JRB transports the largest volume of sediment from the Loess Plateau  
105 to the Yellow River, hydrological studies of the basin have primarily assessed the  
106 impacts of soil and water conservation measures on surface runoff and sediment  
107 transport (e.g., Feng et al., 2012; He et al., 2015; Peng et al., 2015a, 2015b; Wang et al.,  
108 2016). Relatively few studies have been conducted regarding the effects of LULC and  
109 climate changes on runoff. Studies of the Weihe River Basin (Zuo et al., 2014) and

110 Loess Plateau (Liang et al., 2015), which included the JRB as a sub-basin, have  
111 identified the response of runoff to climate change and human activities by using a  
112 climate elasticity model based on the Budyko framework. Zuo et al. (2014) found that  
113 runoff in the JRB decreased by 17.79 mm between 1997 and 2009, with human  
114 activities and climate change accounting for 51% and 39% of this decrease, respectively.  
115 Liang et al. (2015) showed that streamflow decreased substantially from 1961 to 2009,  
116 and the contribution of climate change (65%) to streamflow reduction was much larger  
117 than that of ecological restoration measures (35%) in the JRB. Another study based on  
118 the relationship between precipitation and runoff from 1966 to 1970 showed that runoff  
119 mainly decreased due to precipitation before the 2000s and due to human activity  
120 became dominant thereafter (with a contribution greater than 76%) (Zhang et al., 2011).  
121 The different results reported by Zuo et al. (2014) and Liang et al. (2015) suggest that  
122 assessing the impacts of LULC and climate changes on runoff in relatively large basins  
123 (over 1000 km<sup>2</sup>) is difficult (Chawla and Mujumdar, 2015; Peng et al., 2015b) due to  
124 their complex effects on streamflow (Fu et al., 2007) and the variable boundary  
125 conditions (Chen et al., 2011; Niraula et al., 2015).

126 Therefore, the objectives of this study were as follows: 1) to assess the surface  
127 runoff variability influenced by LULC and climate changes in recent decades in the JRB  
128 by using the SWAT model, which differs from the climate elasticity model based on the  
129 Budyko framework; 2) to quantify the combined and isolated impacts of LULC change  
130 and climate variability on surface runoff in the basin from 1971 to 2005 by using  
131 scenario simulations after calibrating and validating the SWAT model at monthly and

132 yearly time scales; 3) to discuss how LULC and climate changes affect surface runoff;  
133 and 4) to discuss the simulation uncertainty in the context of SWAT modelling due to  
134 parameterizations and provide potential explanations for the conflicting results  
135 regarding the effects of LULC and climate changes on runoff in relatively large basins.

## 136 **2 Methods and materials**

### 137 **2.1 Study area**

138 The JRB, which covers an area of approximately 45421 km<sup>2</sup>, is located at 106°14' –  
139 108°42' E and 34°46' – 37°19' N on the central Loess Plateau in Northwest China (Fig.  
140 1). The main stream of the Jinghe River, with a length of 450 km, originates in the  
141 Liupan Mountains in the Ningxia Autonomous Region and flows across Gansu and  
142 Shanxi Provinces before draining into the Weihe River. The outlet gauging station,  
143 Zhangjiashan, has a control area of approximately 43216 km<sup>2</sup>. The study area is  
144 characterized by hills and syncline valleys, with the Liupan Mountains to the west and  
145 the Ziwu Mountains to the east. The elevation decreases from 2900 m to 360 m above  
146 sea level. The climate varies from sub-humid to semi-arid, with mean annual  
147 precipitation, temperature, and pan evaporation values of 390–560 mm, 8–13 °C, and  
148 1000–1300 mm, respectively. Precipitation mainly occurs between July and September,  
149 accounting for 50–70% of the total annual rainfall.

### 150 **2.2 Runoff change simulation**

151 Under the assumption that runoff is affected only by LULC and climate changes, the  
152 effects of LULC and climate changes on surface runoff were evaluated using SWAT.  
153 Before the simulations, the SWAT model was calibrated and validated as described



154 below.

### 155 **2.2.1 SWAT model and data collection**

156 SWAT, a semi-distributed hydrological model, was developed to assess the impacts of  
157 land management and climate on water, nutrient, and pesticide transport at the basin  
158 scale (Arnold et al., 1998; Neitsch et al., 2005). SWAT simulates hydrological processes  
159 such as surface runoff at the daily time scale based on information regarding weather,  
160 topography, soil properties, vegetation, and land management practices. In SWAT, the  
161 study basin is divided into sub-basins, and each sub-basin is further subdivided into  
162 hydrological response units (HRUs) with homogeneous characteristics (e.g., topography,  
163 soil, and land use). Hydrological components are then calculated in the HRUs based on  
164 the water balance equation.

165 In this study, SWAT is operated via an interface in ArcView GIS (Di Luzio et al.,  
166 2002). Therefore, the required data are either raster or vector data sets, including a  
167 digital elevation model (DEM), soil properties, vegetation, LULC, meteorological  
168 observations, and discharge observations at Zhangjiashan gauging station.

#### 169 (1) DEM

170 The Shuttle Radar Topography Mission (SRTM) 90-m DEM (Jarvis et al., 2008)  
171 was used in this study.

#### 172 (2) Soil data

173 Soil property information was obtained from the soil map of China at a scale of  
174 1:1000000. The map was provided by the Chinese Natural Resources Database.  
175 Huangmiantu, which covers 75.10% of the basin area, is the major soil type in the area

176 according to the Genetic Soil Classification of China. The other seven soil types are  
177 Heilutu (13.27%), Chongjitu (4.30%), Huihetu (3.23%), Hetu (2.41%), Hongniantu  
178 (1.10%), Cugutu (0.35%), and Shandicaodiantu (0.24%).

### 179 (3) Vegetation and LULC data

180 LULC data from four periods were retrieved from Landsat images by supervised  
181 classification, i.e., Multispectral Scanner (MSS) images (60 m resolution) from 1979,  
182 Thematic Mapper (TM) images (30 m resolution) from 1989, and Enhanced Thematic  
183 Mapper Plus (ETM+) images (30 m resolution) from 1999 and 2006. Each LULC  
184 dataset represents the land use patterns for one decade (e.g., LULC data obtained from  
185 1979 represents the land use patterns in the 1970s). Land use was classified into seven  
186 categories: forest, dense grassland, sparse grassland, cropland, water, and barren areas.  
187 Then, the accuracy of the classification was verified, yielding a minimum Kappa  
188 coefficient of 0.73 (Xie et al., 2009).

### 189 (4) Meteorological data

190 Daily precipitation was collected from 16 rainfall stations (Fig. 1), whereas the  
191 daily minimum and maximum temperatures, wind speed, and relative humidity data  
192 required by the SWAT model were collected from 12 meteorological stations between  
193 1970 and 2005. These data were interpolated to DEM grids using the SWAT model's  
194 built-in weather generator, which describes the weather conditions in the model  
195 simulations.

### 196 (5) Surface runoff

197 Daily runoff data measured at the Zhangjiashan gauging station between 1970 and

198 1990 were collected from the State Hydrological Statistical Yearbook. These data were  
199 compared to the modelled surface flow during model calibration and validation.

### 200 2.2.2 Model calibration and validation

201 The SWAT model of the basin was first calibrated for the period of 1971 to 1997 and  
202 was then validated for the period of 1981 to 1990. Based on published results (e.g., Li et  
203 al., 2009) and our previous research results (Qiu et al., 2011), the simulation was the  
204 most sensitive to the following six parameters: runoff curve number ( $CN_2$ ), soil  
205 evaporation compensation factor (ESCO), the available water capacity of the soil layer  
206 (SOL\_AWC), channel conductivity ( $CH_K_2$ ), the baseflow alpha factor (ALPHA\_BF),  
207 and the surface runoff coefficient (SURLAG). Therefore, these six parameters were  
208 calibrated in the SWAT model (Table 1) (Qiu et al., 2011). Model performance was  
209 assessed qualitatively using visual time series plots and quantitatively using the  
210 coefficient of determination ( $R^2$ ) and the Nash-Sutcliffe efficiency coefficient ( $Ens$ ) (Eq.  
211 (1)) (Moriasi et al., 2007).

$$212 \quad Ens = 1 - \frac{\sum_{i=1}^n (Q_{obs} - Q_{sim})^2}{\sum_{i=1}^n (Q_{obs} - Q_{obs\_m})^2} \quad (1)$$

213 where  $Q_{obs}$  and  $Q_{sim}$  are the observed and modelled runoff, respectively;  $Q_{obs\_m}$  is the  
214 mean value of observed runoff; and  $n$  is the number of data records. When  $Ens$   
215 approaches 1, the model simulates the measured data more accurately, whereas a  
216 negative  $Ens$  indicates that the model performance is poor. In this study, a criterion  
217 proposed by Moriasi et al. (2007), the Nash-Sutcliffe coefficient, was adopted to  
218 evaluate the simulation (Table 2).

219 The SWAT model was calibrated and validated based on annual and monthly river  
220 discharges measured at the outlet gauging station shown in Fig. 1.

### 221 **2.2.3 Simulation scenarios**

222 In this study, the effects of LULC and climate changes on surface runoff were evaluated  
223 by comparing the SWAT outputs of ten scenarios. Each scenario represented one decade,  
224 and each simulation required an LULC map and a meteorological data set (Table 3). If  
225 the LULC map and the meteorological data were within the same decade (i.e., the 1970s,  
226 1980s, 1990s, or 2000s), the simulation results represented "real runoff" or a "baseline"  
227 affected by the combination of LULC and climate changes. **Alternatively, varying one**  
228 **driving factor while holding others constant simulated the effects of the variable factor**  
229 **on runoff** (Li et al., 2009). For example, to assess the response of streamflow to  
230 combined LULC and climate changes in the 1970s and 1980s, the simulation of the  
231 1970s (1970–1979) ( $Q_{base, i}$ ), which is used as a reference period or baseline, should be  
232 based on the current LULC (year 1979) and current climate (years 1970–1979). The  
233 simulation of the 1980s (1980–1989) ( $Q_{base, i+1}$ ) should be based on future LULC (year  
234 1989) and future climate (years 1980–1989). The difference between the first and  
235 second simulations represents the combined effects of LULC and climate changes on  
236 streamflow. Regarding LULC changes, the third simulation ( $Q_{sim, cL, i}$ ) was based on the  
237 current climate (years 1970–1979) and the LULC in the next period, or the future LULC  
238 (in this example, 1989). The difference between the first and third simulations is the  
239 effect of the LULC change on streamflow. Similarly, the difference between the first  
240 simulation and the fourth simulation ( $Q_{sim, cc, i}$ ) based on the current LULC (year 1979)

241 and future climate (in this example, 1980–1989) represents the impact of climate change  
 242 on streamflow. The combined effects of LULC and climate changes on streamflow  
 243 ( $\Delta R_{comb}\%$ ) and the isolated effects of LULC ( $\Delta R_{iso, cL}\%$ ) and climate ( $\Delta R_{iso, cc}\%$ ) can be  
 244 assessed using Eqs. (2) to (4).

$$245 \quad \Delta R_{comb}\% = \left( \frac{Q_{base,i+1} - Q_{base,i}}{Q_{base,i}} \right) \times 100 \quad (2)$$

$$246 \quad \Delta R_{iso, cL}\% = \left( \frac{Q_{sim, cL,i} - Q_{base,i}}{Q_{base,i}} \right) \times 100 \quad (3)$$

$$247 \quad \Delta R_{iso, cc}\% = \left( \frac{Q_{sim, cc,i} - Q_{base,i}}{Q_{base,i}} \right) \times 100 \quad (4)$$

## 248 **3 Results**

### 249 **3.1 Climate change**

250 Variations in precipitation, dryness index ( $E_0/P$ , defined as the ratio of annual potential  
 251 evapotranspiration calculated using the Penman–Monteith method to annual  
 252 precipitation), and air temperature were evaluated over four decades based on  
 253 meteorological data from 1970 to 2009 (Fig. 2). Precipitation decreased by 3.4% from  
 254 the 1970s to the 2000s. However, precipitation in the 1980s was slightly higher than that  
 255 in the 1970s. The decreasing trend in precipitation was substantial from the 1980s to the  
 256 1990s, reaching 4.1%. Thereafter, the decrease in precipitation was less than that from  
 257 1980 to 1999. During the entire period (from the 1970s to the 2000s), the temperature  
 258 increased by 13.6% (1.18 °C), including an abrupt increase of 0.7 °C from the 1980s to  
 259 the 1990s. Although the dryness index exhibited little change (increasing by 1.8%), a  
 260 large dryness index ( $>1.9$ ) indicates that the climate became drier. These results indicate  
 261 that the climate in the JRB changed dramatically over the last four decades, as

262 characterized by decreased precipitation and increased temperature and dryness index  
263 values. Both warming and drying trends are evident in the JRB. These results agree with  
264 the results of other studies that reflect a broader phenomenon known as “climatic  
265 warming and drying” in northern China (Ma and Fu, 2003; Huang et al., 2012).

### 266 **3.2 LULC change**

267 Figure 3 shows the variations in LULC distributions over the last four decades. The  
268 dominant land-use types are sparse grassland (with a vegetation coverage of  $< 20\%$ ) and  
269 cropland, which encompass a total of  $> 61\%$  of the area over the four decades. However,  
270 the percentage of sparse grassland was slightly higher than that of cropland, and the  
271 margin varied from 2.96% to 9.80%. The remaining types include dense grassland (with  
272 a vegetation coverage of  $\geq 20\%$ ), forest, barren areas, urban and built-up areas, and  
273 water, with mean ratios of 17.57%, 13.71%, 6.35%, 0.31%, and 0.29%, respectively.  
274 The vegetation with low coverage that is predominant in the study basin corresponds  
275 with the regional climate, and the relatively high percentage of cropland indicates the  
276 importance of agriculture in this area.

277 The statistical results illustrated by the four LULC maps over the last four decades  
278 indicate that vegetation (including grassland and forest) decreased by 11% between the  
279 1970s and the 1990s and increased by 6% thereafter. The areas of cropland and urban  
280 and built-up areas increased by 4.03% and 0.95%, respectively, over time. The area of  
281 water fluctuated slightly, increasing by 0.09%. The area of barren land increased from  
282 3.09% to 12.35% before the 1990s but then decreased to 3.02% in the 2000s. The  
283 LULC changes potentially resulted from two major factors: social development and

284 population growth. These factors have increased since the 1980s, leading to the  
285 expansion of urban and agricultural activities as well as unreasonable land utilization,  
286 reclamation of vulnerable land, and vegetation removal. Therefore, the areas of urban  
287 and barren land increased while the area of vegetation decreased. However, the  
288 decreasing trend in vegetation changed due to a nationwide environmental conservation  
289 programme initiated in 1999 by the Chinese government, the **Grain for Green Program**  
290 **(GGP)** (Xu et al., 2004). The main goal of the **GGP** was to reduce soil erosion and  
291 improve the eco-environmental status of western and northern China (Xu et al., 2004).  
292 Noticeable evidence of ecological restoration was observed on the Loess Plateau after  
293 the **GGP** was implemented (Chang et al., 2011; Sun et al., 2015). In addition to  
294 preventing soil erosion, the **GGP** improved the soil physical and chemical properties  
295 (Deng et al., 2014; Song et al., 2014) and facilitated vegetation restoration. The results  
296 indicate that vegetation increased since the late 1990s, and these results agree with the  
297 results of other studies (e.g., Liang et al., 2015; Wang et al., 2016).

### 298 **3.3 Performance of the SWAT model**

299 The SWAT model performed well in both the calibration and validation periods,  
300 accurately simulating the outlet flows according to the model performance criteria ( $R^2$   
301 and *Ens*) after the six sensitive parameters were optimized. During the calibration  
302 period (1971–1980), the time series plots of simulations and observations were similar  
303 at both the annual (Fig. 4 (a)) and monthly scales (Fig. 5 (a)), although overestimation  
304 was observed in the simulated streamflow. Point-by-point comparisons between the  
305 simulations and observations further showed that most of the paired streamflow values

306 were distributed near the 1:1 line, with mean  $R^2$  values of 0.90 (Fig. 4 (b)) and 0.84 (Fig.  
307 5 (b)) at the annual and monthly scales, respectively (Qiu et al., 2011). In addition, the  
308 results of a statistical analysis indicated that the mean *Ens* values were 0.76 and 0.72 at  
309 the annual and monthly scales, respectively (Table 4). Similarly, although the SWAT  
310 model did not perform as well during the validation period (1981–1990) relative to the  
311 calibration period, the performance was still adequate, with *Ens* ( $R^2$ ) values of 0.73  
312 (0.83) and 0.69 (0.77) at the annual and monthly scales, respectively (Table 4, Figs. 6  
313 and 7).

314 Although the *Ens* performance statistic associated with SWAT runoff modelling  
315 can be larger than 0.8 in small or humid basins (e.g., Luo et al., 2008; Qiao et al., 2015;  
316 Wu et al., 2016), *Ens* is typically less than 0.7 in relatively large river basins in arid to  
317 semi-arid regions (e.g., Xu et al., 2011; Notter et al., 2013; Zhang et al., 2015; Liu et al.,  
318 2016; Zhao et al., 2016). The *Ens* values in this study were generally good in the  
319 calibration and validation periods and were comparable to those reported in other  
320 studies in arid to semi-arid river basins. The results suggested that the SWAT model  
321 performed well and was applicable to the study basin.

### 322 **3.4 Simulated surface runoff**

323 The annual runoff simulated by SWAT under different scenarios is shown in Table 3.  
324 Generally, runoff increased minimally between the 1970s and the 2000s at a rate of 1.51  
325  $\text{m}^3 \text{s}^{-1}$  (simulations S1 and S10) due to the combined effects of LULC and climate  
326 changes (Fig. 8). However, runoff changed differently in different decades. For example,  
327 runoff increased by 35.4% ( $29.75 \text{ m}^3 \text{ s}^{-1}$ ) from the 1970s to the 1980s (simulations S1



328 and S4) but decreased thereafter. Notably, the simulated runoff in the 1990s was 12.59  
329  $\text{m}^3 \text{s}^{-1}$  less than that in the 1980s (simulations S4 and S7), and runoff decreased by  
330 15.5% ( $15.65 \text{ m}^3 \text{ s}^{-1}$ ) from the 1990s to the 2000s (simulations S7 and S10) (Table 3).

## 331 **4 Discussion**

### 332 **4.1 Impacts of LULC and climate changes on surface runoff**

333 The hydrological effects were analysed using the simulated runoff data rather than the  
334 observed data. The combined effects of LULC and climate changes on surface runoff  
335 are presented in section 3.4. The simulated runoff increased between the 1970s and the  
336 1980s, while precipitation increased from 521 mm to 527 mm during the same period.  
337 Thereafter, runoff decreased as precipitation decreased. However, runoff decreased by  
338 11.1% from the 1980s to the 1990s but decreased by 15.5% from the 1990s to the 2000s.  
339 These results indicate that, although precipitation can considerably affect runoff  
340 simulation, variations in runoff and precipitation were nonlinear due to the combined  
341 effects.

342 The isolated impacts of LULC and climate changes on surface runoff can be  
343 analysed by comparing two sets of simulations. The differences between S1 and S2 (as  
344 well as between S4 and S5 and S7 and S8) reflect the impacts of climate change on  
345 runoff. Accordingly, the differences between S1 and S3 (as well as between S4 and S6  
346 and S7 and S9) reflect the impacts of climate change on runoff.

#### 347 **4.1.1 Isolated impacts of LULC change**

348 During the first two decades, LULC changes increased runoff by  $2.30 \text{ m}^3 \text{ s}^{-1}$  and  
349 accounted for 7.73% of the total change ( $29.75 \text{ m}^3 \text{ s}^{-1}$ ). Thereafter, LULC change

350 decreased runoff by  $6.83 \text{ m}^3 \text{ s}^{-1}$ , which accounted for 54.25% of the total change in  
351 runoff ( $12.59 \text{ m}^3 \text{ s}^{-1}$ ) from the 1980s to the 1990s. The impacts of LULC changes on  
352 runoff increased during the last two decades because the contribution of LULC changes  
353 to runoff increased to 70.67% from the 1990s to the 2000s (Fig. 9).

354 The results in section 3.2 show that the LULC changed slightly from the 1970s to  
355 the 1980s. For example, the area of cropland marginally increased by 0.76%, and the  
356 vegetative area decreased by 3.19%. This small LULC change indicates that human  
357 activities minimally influenced runoff during the first two decades because the LULC  
358 changes only accounted for 7.73% of the increase in runoff. However, the LULC  
359 changed considerably with social development and population growth beginning in the  
360 1980s. The vegetative area decreased by 7.81% from the 1980s to the 1990s, and the  
361 percentages of cropland, barren areas, and urban and built-up areas increased by 2.39%,  
362 5.43%, and 0.11%, respectively. LULC changes associated with increased human  
363 activities accounted for 54.25% of the increase in surface runoff. Furthermore, the GGP,  
364 which was initiated in the late 1990s, mitigated the decreasing trend in vegetation.  
365 Although cropland and urban and built-up areas still expanded by 2.40% and 0.82%,  
366 respectively, from the 1990s to the 2000s, vegetation increased by 6.00%, and barren  
367 areas decreased by 9.33%. Therefore, LULC change exhibited a relatively large  
368 influence on the surface runoff change, contributing to 70.67% of the surface runoff in  
369 the last two decades.

370 In addition, the spatial distributions of different land use types influence the  
371 generation of runoff. As reported in our previous publication (Qiu et al., 2011), the soil

372 moisture content and evapotranspiration were modified by LULC changes (i.e., the  
373 GGP) after the GGP in the JRB, which led to changes in surface runoff. However, the  
374 modification was different. Fig. 10 shows that, after the GGP, the soil moisture content  
375 increased in the three selected sub-basins from the upstream to downstream regions,  
376 while the runoff and evapotranspiration decreased. When considering the upstream area  
377 as an example, barren land, with an initial percentage of 15.90%, and partial farmland,  
378 with an initial percentage of 6.56%, were converted to grassland due to the GGP, which  
379 improved water filtration and increased the soil moisture (Fig. 10 (a)). The simulation in  
380 Fig. 10 shows that the soil moisture content increased by 163.66%, 208.23%, and  
381 262.66% in the sub-basins from the upstream to downstream, whereas the surface runoff  
382 (evapotranspiration) decreased by -37.53%, -38.55%, and -49.01% (-1.21%, -3.06%,  
383 and -25.90%), respectively. These results indicate that the impacts of LULC changes on  
384 flow regimes were larger in the downstream areas of the basin than in the upstream  
385 areas.

386 Although climate variables were held constant when simulating LULC changes,  
387 the isolated influences of LULC changes on runoff did not exclude the impacts of  
388 precipitation variations because the climate (including precipitation) varied in each  
389 decade (Table 3). Nonetheless, the above results indicate that LULC changes  
390 contributed considerably to decreased runoff, as reported in previous studies (e.g.,  
391 Zhang et al., 2011; Zuo et al., 2014; Wang et al., 2014b; Wang et al., 2016). Additionally,  
392 the results suggest that vegetation restoration due to the GGP reduced surface runoff,  
393 which agrees with the results of other studies (e.g., Li et al., 2009; Nunes et al., 2011).

#### 394 **4.1.2 Isolated impacts of climate change**

395 Unlike the contributions of LULC changes, the influences of climate change decreased  
396 in recent decades (Fig. 9). Climate change increased runoff by  $26.07 \text{ m}^3 \text{ s}^{-1}$  from the  
397 1970s to the 1980s, accounting for approximately 87.63% of the increased total runoff  
398 during that period. Since the 1980s, surface runoff decreased, and the contributions of  
399 climate change to decreased runoff were 55.92% and 42.11% from the 1980s to the  
400 1990s and from the 1990s to the 2000s, respectively. The influence of climate change on  
401 runoff agrees with climatic warming and drying trends. Decreasing precipitation will  
402 potentially lead to less runoff, whereas increasing temperatures will result in increased  
403 evaporation.

404 In summary, LULC and climate changes accounted for 7.73% and 87.63% of the  
405 total runoff increase ( $29.75 \text{ m}^3 \text{ s}^{-1}$ ) in the 1970s and 1980s, respectively. The isolated  
406 influences of LULC and climate changes on runoff were nearly the same from 1980 to  
407 1999 (54.25% and 55.92%, respectively) compared to the total decrease in runoff. In the  
408 last two decades, the percentage of the total runoff decrease that was caused by LULC  
409 changes (70.67%) was greater than that caused by climate change (42.11%).

410 Although uncertainties exist in the simulations (see section 4.2 for details), the  
411 above results indicate that the contribution of climate variability decreased over the last  
412 four decades, while the contribution of LULC change increased. Unlike the results  
413 reported by Liang et al. (2015), the findings in this study suggested that runoff  
414 fluctuations are influenced less by climate change and more by human activities. The  
415 results also indicate that the impacts of human activities on runoff have gradually

416 increased in the JRB, which agrees with the results of other studies (Zhang et al., 2011;  
417 Zuo et al., 2014; Wang et al., 2016).

#### 418 **4.2 Uncertainty in SWAT model simulations**

419 Uncertainty in model simulations, which is mainly caused by model structure (e.g.,  
420 algorithm limitations) and model parameterizations, is a major challenge when  
421 assessing the impacts of LULC and climate changes on runoff in relatively large basins.  
422 In this study, the SWAT model performed well, with a Nash-Sutcliffe efficiency  
423 coefficient and coefficient of determination of 0.76 and 0.90, respectively, for annual  
424 runoff during the calibration period, as well as values of 0.73 and 0.83, respectively,  
425 during the validation period. However, under the assumption that runoff is affected only  
426 by LULC or climate changes, the simulated runoff associated with changes in only one  
427 driving factor was slightly different than the simulated runoff obtained when  
428 considering the combined effects of both factors due to the uncertainty in representing  
429 LULC and climate change interactions in the SWAT model. For example,  $28.37 \text{ m}^3 \text{ s}^{-1}$ ,  
430 which was the combined runoff rate in S2 and S3, was not equal to the "real or baseline  
431 runoff" of  $29.75 \text{ m}^3 \text{ s}^{-1}$  in S4.

432 Qiao et al. (2015) reported that the SWAT model performed much better in small  
433 watersheds (2–5 ha) than in a larger watershed ( $78 \text{ km}^2$ ) because the meteorological  
434 inputs (e.g., precipitation) do not represent the spatial variability in a given parameter  
435 over larger basins because ground-based observations are limiting. To reduce the  
436 uncertainty and improve the accuracy of the hydrological model and forecasting results  
437 for relatively large basins, **the uncertainty associated with model parameterization is**

438 discussed below and potential solutions are proposed for future studies.

439 In this study, the basin area exceeded 45000 km<sup>2</sup>. However, only 16 rainfall  
440 stations were available, among which six stations were outside the study basin. The  
441 station density was 0.35 stations per 1000 km<sup>2</sup>. Xu et al. (2013) found that model  
442 simulations are influenced by rainfall station densities below 0.4 per 1000 km<sup>2</sup>. Under  
443 such conditions, runoff simulations may contain uncertainties due to poor representation  
444 of spatial precipitation variability, which is crucial in determining the runoff hydrograph  
445 (Singh, 1997). Previous studies (e.g., Chu et al., 2011; Masih et al., 2011; Shope and  
446 Maharjan, 2015) have suggested that the density of rainfall measurement stations has a  
447 significant impact on SWAT simulations and that reducing the precipitation uncertainty  
448 can improve the accuracy of simulated streamflows. Although the SWAT model  
449 performed well in this study and the uncertainty in the simulations associated with  
450 precipitation was similar to the uncertainties observed in other studies, peak flow  
451 overestimation was observed in the simulated runoff (Figs. 4 to 7). To reduce  
452 uncertainty, precipitation from stations should be processed (e.g., via interpolation)  
453 before conducting runoff simulations, thereby improving the precision and spatial  
454 representativeness, especially in relatively large basins without reliable and precise areal  
455 rainfall data.

456 In addition, the coarse vegetation information provided by the LULC data in this  
457 study can lead to uncertainty in the simulations because vegetation distinction is  
458 required in SWAT modelling. Although the LULC data had a relatively high resolution  
459 of 30 m, we can only provide a general vegetation categorization, such as forest, due to

460 the data limitations. Recent results (e.g., Pierini et al., 2014; Qiao et al., 2015) have  
461 shown that detailed biophysical parameters of vegetation species can improve the  
462 performance of distributed, physically based models such as SWAT and reduce model  
463 uncertainty. In China, detailed and reliable data related to vegetation species are  
464 uncommon. Reliable maps of vegetation species (as well as other geographic maps) at  
465 high spatial resolutions (e.g., <1000 m) are an urgently needed to provide detailed and  
466 heterogeneous information for accurate biophysical and hydrological parameterization.

## 467 **5 Conclusions**

468 In this study, the SWAT model was used to simulate the effects of LULC and climate  
469 changes on surface runoff. The satisfactory performance of the SWAT model was  
470 confirmed by the Nash-Sutcliffe coefficient and coefficient of determination values of  
471 annual runoff of 0.76 and 0.90, respectively, during the calibration period and 0.73 and  
472 0.83, respectively, during the validation period. Simulations showed that the combined  
473 effects of LULC and climate changes increased surface runoff by  $29.75 \text{ m}^3 \text{ s}^{-1}$  during  
474 the 1970s and the 1980s, whereas LULC and climate changes both decreased runoff by  
475  $28.24 \text{ m}^3 \text{ s}^{-1}$  during the 1980s and the 2000s. Further analysis suggested that different  
476 driving factors had different influences on surface runoff.

477 The isolated results indicated that the impacts of LULC changes on the  
478 hydrological cycle were gradual, and that LULC changes altered runoff to a similar or  
479 greater extent than climate change, accounting for 70.67% of the streamflow reduction  
480 since the late 1990s. This result suggests that LULC plays an important role in the  
481 transition zone between semi-humid and semi-arid regions. As an indicator that is

482 closely related to human activities, the LULC in the study area underwent considerable  
483 changes, especially the vegetation cover rate, which decreased by 16% from the 1970s  
484 to the 1990s and increased by 6% between the 1990s and the 2000s due to the **Grain for**  
485 **Green Program (GGP)**. In conclusion, the increased vegetation and land use changes  
486 inevitably altered the hydrological cycle, and large-scale LULC changes under the **GGP**  
487 considerably affected the hydrological cycle.

488 To reduce simulation uncertainty and improve the accuracy of hydrological  
489 modelling and forecasting in relatively large basins, areal input parameters (e.g.,  
490 precipitation and **vegetation species information**) **should be generated with reliable**  
491 **precision and high spatial resolution.**

#### 492 **Acknowledgements**

493 This study was supported by the National Natural Science Foundation of China  
494 (Nos. 51309246 and 31300402), the China Scholarship Council (No. 201606380186),  
495 and the National Basic Research Program of China (project No. 2006CB400505). We  
496 thank the China Meteorological Administration for providing meteorological data. **We**  
497 **are grateful to the editors and reviewers for their insightful and constructive comments.**

#### 498 **References**

499 Arnold, J. G., Srinivasan, R., Muttiah, R. S., and Williams, J. R.: Large area hydrologic  
500 modeling and assessment-Part 1: Model development, Journal of the American Water  
501 Resources Association, 34, 73–89, 1998.

502 Chang, R. Y., Fu, B. J., Liu, G. H., and Liu, S.G.: Soil carbon sequestration potential for



503 Grain for Green Project in Loess Plateau, China, *Environmental Management*, 48,  
504 1158–1172, 2011.

505 Chawla, I., and Mujumdar, P. P.: Isolating the impacts of land use and climate change on  
506 streamflow, *Hydrology and Earth System Sciences*, 19, 3633–3651, 2015.

507 Chen, Y., Li, J., and Xu, H. J.: Improving flood forecasting capability of physically  
508 based distributed hydrological model by parameter optimization, *Hydrology and  
509 Earth System Sciences*, 20, 375–392, 2016.

510 Chen, Y., Ren, Q. W., Huang, F. H., Xu, H. J., and Cluckie, I.: Liuxihe Model and its  
511 modeling to river basin flood, *Journal of Hydrologic Engineering*, 16, 33–50, 2011.

512 Chu, J., Zhang, C., Wang, Y., Zhou, H., and Shoemaker, C. A.: A watershed rainfall data  
513 recovery approach with application to distributed hydrological models, *Hydrological  
514 Processes*, 26, 1937–1948, 2012.

515 D'Agostino D. R., Trisorio, L. G., Lamaddalena, N., and Ragab, R.: Assessing the results  
516 of scenarios of climate and land use changes on the hydrology of an Italian catchment:  
517 modelling study, *Hydrological Processes*, 24, 2693–2704, 2010.

518 Deng, L., Liu, G. B., and Shangguan, Z. P.: Land use conversion and changing soil  
519 carbon stocks in China's 'Grain-for-Green' Program': a synthesis, *Global Change  
520 Biology*, 20, 3544–3556, 2014.

521 Di Luzio, M., Srinivasan, R., Arnold, J. G., and Neitsch, S. L.: ArcView Interface for  
522 SWAT2000, User's Guide. Temple, Tex.: Texas A&M Agricultural Experiment Station,  
523 Blackland Research and Extension Center, 2002.

524 Fan, M., and Shibata, H.: Simulation of watershed hydrology and stream water quality

525 under land use and climate change scenarios in Teshio River watershed, northern  
526 Japan, *Ecological Indicators*, 50, 79–89, 2015.

527 Feng, X. M., Sun, G., Fu, B. J., Su, C. H., Liu, Y., and Lamparski, H.: Regional effects  
528 of vegetation restoration on water yield across the Loess Plateau, China, *Hydrology  
529 and Earth System Sciences*, 16, 2617–2628, doi:10.5194/hess-16-2617-2012, 2012.

530 Foley, J. A., DeFries, R., Asner, G. P., Barford, C., Bonan, G., Carpenter, S. R., Chapin, F.  
531 S., Coe, M. T., Daily, G. C., and Gibbs, H. K.: Global consequences of land use,  
532 *Science*, 309, 570–574, 2005.

533 Fu, C. B.: Potential impacts of human-induced land cover change on East Asia monsoon,  
534 *Global and Planetary Change*, 37, 219–229, 2003.

535 Fu, G., Charles, S. P., and Chiew, F. H. S.: A two-parameter climate elasticity of  
536 streamflow index to assess climate change effects on annual streamflow, *Water  
537 Resources Research*, 43, W11419, 2007.

538 Gassman, P., Reyes, M. R., Green, C. H., and Arnold, J.G.: The soil and water  
539 assessment tool: Historical development, applications, and future research directions,  
540 *Transactions of the ASABE*, 50, 1211–1250, 2007.

541 Guo, H., Qi, H., and Jiang, T.: Annual and seasonal streamflow responses to climate and  
542 land-cover changes in the Poyang Lake basin, *Journal of Hydrology*, 355, 106–122,  
543 2008.

544 He, Y., Wang, F., Mu, X. M., Yan, H. T., and Zhao, G. J.: An Assessment of Human  
545 versus Climatic Impacts on Jing River Basin, Loess Plateau, China, *Advances in  
546 Meteorology*, 2015, 478739, 2015.

547 Huang, J., Guan, X., and Ji, F.: Enhanced cold-season warming in semi-arid regions,  
548 Atmospheric Chemistry and Physics, 12, 5391–5398, 2012.

549 IPCC: Climate change 2007: the physical science basis, in: Contribution of working  
550 group I to the fourth assessment report of the intergovernmental panel on climate  
551 change, edited by: Solomon, S., Qin, D., Manning, M., Chen, Z., Marquis, M., Averyt,  
552 K. B., Tignor, M., and Miller, H. L., Cambridge University Press, Cambridge, UK,  
553 2007.

554 Jarvis, A., Reuter, H. I., Nelson, A., Guevara, E.: Hole-filled SRTM for the globe  
555 Version 4, available from the CGIAR-CSI SRTM 90m Database at:  
556 <http://srtm.csi.cgiar.org> , 2008 (last access: 24 October 2015).

557 Jiang, S., Ren, L., Yong, B., Singh, V. P., Yang, X., and Yuan, F.: Quantifying the effects  
558 of climate variability and human activities on runoff from the Laohahe basin in  
559 northern China using three different methods, Hydrol. Process., 25, 2492–2505, 2011.

560 Jiang, T., Chen, Y. Q., Xu, C. Y., Chen, X. H., Chen, X., and Singh, V. P.: Comparison of  
561 hydrological impacts of climate change simulated by six hydrological models in the  
562 Dongjiang Basin, South China, Journal of Hydrology, 336, 316–333, 2007.

563 Krysanova, V, and Arnold, J. G.: Advances in ecohydrological modelling with SWAT – a  
564 review, Hydrological Sciences Journal, 53, 939–947, 2008.

565 Krysanova, V, and Arnold, J. G.: Advances in water resources assessment with  
566 SWAT—an overview, Hydrological Sciences Journal, 60, 771–783, 2015.

567 Leavesley, G. H.: Modeling the effects of climate change on water resources: A review,  
568 Climate Change, 28, 159–177, 1994.

569 Leng, G., Tang, Q., Huang, S., Zhang, X., and Cao, J.: Assessments of joint hydrological  
570 extreme risks in a warming climate in China, *International Journal of Climatology*, 36,  
571 1632–1642, 2016.

572 Li, J., Chen, F., Cook, E. R., Gou, X., and Zhang, Y.: Drought reconstruction for North  
573 Central China from tree rings: the value of the Palmer drought severity index,  
574 *International Journal of Climatology*, 27, 903–909, 2007.

575 Li, M. X., Ma, Z. G., and Niu, G. Y.: Modeling spatial and temporal variations in soil  
576 moisture in China, *Chin. Sci. Bull.*, 56, 1809–1820, 2011.

577 Li, Z., Liu, W. Z., Zhang, X. C., and Zheng, F. L.: Impacts of land use change and  
578 climate variability on hydrology in an agricultural catchment on the loess plateau of  
579 China, *Journal of Hydrology*, 377, 35–42, 2009.

580 Li, Z., Zheng, F. L., Liu, W. Z., and Flanagan, D. C.: Spatial distribution and temporal  
581 trends of extreme temperature and precipitation events on the Loess Plateau of China  
582 during 1961–2007, *Quaternary International*, 226, 92–100, 2010.

583 Liang, W., Bai, D., Wang, F., Fu, B., Yan, J., Wang, S., Yang, Y., Long, D., and Feng M.:  
584 Quantifying the impacts of climate change and ecological restoration on streamflow  
585 changes based on a Budyko hydrological model in China's Loess Plateau, *Water  
586 Resources Research*, 51, 6500–6519, doi:10.1002/2014WR016589, 2015.

587 Liu, J., Liu, T., Bao, A. M., De Maeyer, P., Feng, X. W., Miller, S. N., and Chen, X.:  
588 Assessment of Different Modelling Studies on the Spatial Hydrological Processes in  
589 an Arid Alpine Catchment, *Water Resources Management*, 30, 1757–1770, 2016.

590 Liu, X. P., Li X.: Simulating complex urban development using kernel-based non-linear

591 cellular automata, *Ecological Modelling*, 211 (1–2), 169–181, 2008.

592 Luo, Y., Zhang, X., Liu, X., Ficklin, D., and Zhang, M.: Dynamic modeling of  
593 organophosphate pesticide load in surface water in the northern San Joaquin Valley  
594 watershed of California, *Environmental Pollution*, 156, 1171–1181, 2008.

595 Ma, Z. G., and Fu, C. B.: Interannual characteristics of the surface hydrological  
596 variables over the arid and semi-arid areas of northern China, *Global and Planetary  
597 Change*, 37, 189–200, 2003.

598 Ma, Z., and Fu, C.: Some evidence of drying trend over northern China from 1951 to  
599 2004, *Chinese Science Bulletin*, 51, 2913–2925, 2006.

600 Ma, Z., Kang, S., Zhang, L., Tong, L., and Su, X.: Analysis of impacts of climate  
601 variability and human activity on streamflow for a river basin in arid region of  
602 northwest China, *Journal of Hydrology*, 352, 239–249, 2008.

603 Masih, I., Maskey, S., Uhlenbrook, S., and Smakhtin, V.: Assessing the Impact of Areal  
604 Precipitation Input on Streamflow Simulations Using the SWAT Model, *Journal of  
605 the American Water Resources Association*, 47, 179–195, 2011.

606 Milly, P. C. D., Dunne, K. A., and Vecchia, A. V.: Global pattern of trends in streamflow  
607 and water availability in a changing climate, *Nature*, 438, 347–350, 2005.

608 Moriasi, D. N., Arnold, J. G., van Liew, M. W., Binger, R. L. Harmel, R. D., and Veith,  
609 T.: Model evaluation guidelines for systematic quantification of accuracy in  
610 watershed simulations, *Transactions of the ASABE*, 50, 885–900, 2007.

611 Murray, S. J., Foster, P. N., and Prentice, I. C.: Future global water resources with  
612 respect to climate change and water withdrawals as estimated by a dynamic global

613 vegetation model, *Journal of Hydrology*, 448–449, 14–29, 2012.

614 Neitsch, S. L., Arnold, J. G., Kiniry, J. R., and Williams, J. R.: Soil and Water  
615 Assessment Tool Theoretical Documentation. Ver. 2005. Temple, Tex.: USDA - ARS  
616 Grassland Soil and Water. Research Laboratory, and Texas A&M University,  
617 Blackland Research and Extension Center, 2005.

618 Niraula, R., Meixner, T., and Norman, L. M.: Determining the importance of model  
619 calibration for forecasting absolute/relative changes in streamflow from LULC and  
620 climate changes, *Journal of Hydrology*, 522, 439–451, 2015.

621 Notter, B., Hans, H., Wiesmann, U., and Ngana, J. O.: Evaluating watershed service  
622 availability under future management and climate change scenarios in the Pangani  
623 Basin, *Physics and Chemistry of the Earth*, 61–62, 1–11, 2013.

624 Nunes, A. N., de Almeida, A. C., and Coelho C. O. A.: Impacts of land use and cover  
625 type on runoff and soil erosion in a marginal area of Portugal, *Applied Geography*, 31,  
626 687–699, 2011.

627 Oki, T., and Kanae, S.: Global hydrological cycles and world water resources, *Science*,  
628 313, 1068–1072, 2006.

629 Olivera, F., and DeFee, B. B.: Urbanization and its effect on runoff in the Whiteoak  
630 Bayou watershed, Texas, *Journal of the American Water Resources Association*, 43,  
631 170–182, 2007.

632 Peng, H., Jia, Y. W., Qiu, Y. Q., and Niu, C. W.: Assessing climate change impacts on  
633 the ecohydrology of the Jinghe River basin in the Loess Plateau, China, *Hydrological  
634 Sciences Journal*, 58 (3), 651–670, 2013.

635 Peng, H., Jia, Y., Niu, C. W., Gong, J. G., Hao, C. F., Gou, S.: Eco-hydrological  
636 simulation of soil and water conservation in the Jinghe River Basin in the Loess  
637 Plateau, China, *Journal of Hydro-environment Research*, 9 (3), 452–464, 2015b.

638 Peng, H., Jia, Y., Tague, C., and Slaughter, P.: An Eco-Hydrological Model-Based  
639 Assessment of the Impacts of Soil and Water Conservation Management in the Jinghe  
640 River Basin, China, *Water*, 7, 6301–6320, 2015a.

641 Piao, S., Friedlingstein, P., Ciais, P., de Noblet-Ducoudré, N., Labat, D., and Zaehle, S.:  
642 Changes in climate and land use have a larger direct impact than rising CO<sub>2</sub> on global  
643 river runoff trends, *PNAS*, 104, 15242–15247, 2007.

644 Pierini, N., Vivoni, E., Robles-Morua, A., Scott, R., and Nearing, M.: Using  
645 observations and a distributed hydrologic model to explore runoff thresholds linked  
646 with mesquite encroachment in the Sonoran Desert, *Water Resources Research*, 50,  
647 8191–8215, 2014.

648 Praskievicz, S., and Chang, H.: A review of hydrological modeling of basin-scale  
649 climate change and urban development impacts, *Progress in Physical Geography*, 33,  
650 650–671, 2009.

651 Qiao, L., Zou, C., Will, R., and Stebler, E.: Calibration of SWAT model for woody plant  
652 encroachment using paired experimental watershed data, *Journal of Hydrology*, 523,  
653 231–239, 2015.

654 Qiu, G. Y., Yin, J., Geng, S.: Impact of climate and land-use changes on water security  
655 for agriculture in Northern China, *Journal of Integrative Agriculture*, 11, 144–150,  
656 2012.

657 Qiu, G. Y., Yin, J., Tian, F., and Geng, S.: Effects of the "Conversion of Cropland to  
658 Forest and Grassland Program" on the water budget of the Jinghe River Catchment in  
659 China, *Journal of Environmental Quality*, 40, 1–11, 2011.

660 Sherwood, S., and Fu, Q.: A drier future, *Science*, 343, 737–739, 2014.

661 Shope, C. L., and Maharjan, G. R.: Modeling Spatiotemporal Precipitation: Effects of  
662 Density, Interpolation, and Land Use Distribution, *Advances in Meteorology*, 2015,  
663 174196, 16 pages, 2015.

664 Singh, V. P.: Effect of spatial and temporal variability in rainfall and watershed  
665 characteristics on stream flow hydrograph, *Hydrological Processes*, 11, 1649–1669,  
666 1997.

667 Song, X., Peng, C., Zhou, G., Jiang, H., and Wang, W.: Chinese Grain for Green  
668 Program led to highly increased soil organic carbon level: A meta-analysis, *Scientific*  
669 *Reports*, 4, 4460, 2014.

670 Sterling, S. M., Ducharme, A., and Polcher, J.: The impact of global land-cover change  
671 on the terrestrial water cycle, *Nature Climate Change*, 3, 385–390, 2012.

672 Sun, W., Song, X., Mu, X., Gao, P., Wang, F., and Zhao, G.: Spatiotemporal vegetation  
673 cover variations associated with climate change and ecological restoration in the  
674 Loess Plateau, *Agricultural and Forest Meteorology*, 209–210, 87–99, 2015.

675 Vigerstol, K., and Aukema, J. E.: A comparison of tools for modeling freshwater  
676 ecosystem services, *Journal of Environmental Management*, 92, 2403–2409, 2011.

677 Vorosmarty, C. J., McIntyre, P. B., Gessner, M. O., Dudgeon, D., Prusevich, A., Green,  
678 P., Glidden, S., Bunn, S. E., Sullivan, C. A., Reidy Liermann, C., and Davies, P. M.:



679 Global threats to human water security and river biodiversity, *Nature*, 467, 555–561,  
680 2010.

681 Wang, G., and Cheng, G.: The characteristics of water resources and the changes of the  
682 hydrological process and environment in the arid zone of northwest China,  
683 *Environmental Geology*, 39, 783–790, 2000.

684 Wang, G., Yang, H., Wang, L., Xu, Z., Xue, B.: Using the SWAT model to assess  
685 impacts of land use changes on runoff generation in headwaters, *Hydrological  
686 Processes*, 28, 1032–1042, 2014b.

687 Wang, G., Yu, J., Shrestha, S., Ishidaira, K., and Takeuchi, H.: Application of a  
688 distributed erosion model for the assessment of spatial erosion patterns in the Lushi  
689 catchment, China, *Environmental Earth Sciences*, 61 (4), 787–797, 2010.

690 Wang, R., Kalin, L., Kuang, W., and Tian, H.: Individual and combined effects of land  
691 use/cover and climate change on Wolf Bay watershed streamflow in southern  
692 Alabama, *Hydrological Processes*, 28, 5530–5546, 2014a.

693 Wang, S., Fu, B. J., Piao, S. L., Lu, Y. H., Ciais, P., Feng, X. M., and Wang, Y. F.:  
694 Reduced sediment transport in the Yellow River due to anthropogenic changes,  
695 *Nature Geoscience*, 9, 38–41, 2016.

696 Wei, S., Yang, H., Song, J., Abbaspour, K. C., Xu, Z.: System dynamics simulation  
697 model for assessing socio-economic impacts of different levels of environmental flow  
698 allocation in the Weihe River Basin, China, *European Journal of Operational  
699 Research*, 221, 248–262, 2012.

700 Wu, W., Xu, Z. X., Yin, X., W., and Zuo, D. P.: Assessment of ecosystem health based

701 on fish assemblages in the Wei River basin, China, *Environmental Monitoring and*  
702 *Assessment*, 186 (6), 3701–3716, 2014.

703 Wu, Y. P., Liu, S. G., Yan, W. D., Xia, J. Z., Xiang, W. H., Wang, K. L., Luo, Q., Fu, W.,  
704 and Yuan, W. P.: Climate change and consequences on the water cycle in the humid  
705 Xiangjiang River Basin, China, *Stochastic Environmental Research and Risk*  
706 *Assessment*, 30, 225–235, 2016.

707 Xie, F., Qiu, G. Y., Yin, J., Xiong, Y. J., and Wang, P.: Comparison of land use/land  
708 cover change in three sections of the Jinghe River basin between the 1970s and 2006,  
709 *Journal of Natural Resources*, 24 (8), 1354–1365, 2009. (in Chinese with English  
710 abstract)

711 Xu, H., Taylor, R. G., and Xu, Y.: Quantifying uncertainty in the impacts of climate  
712 change on river discharge in sub-catchments of the Yangtze and Yellow River Basins,  
713 *China, Hydrology and Earth System Sciences*, 15, 333–344, 2011.

714 Xu, H., Xu, C. Y., Chen, H., Zhang, Z., and Li, L.: Assessing the influence of rain gauge  
715 density and distribution on hydrological model performance in a humid region of  
716 China, *Journal of Hydrology*, 505, 1–12, 2013.

717 Xu, Z., Bennett, M. T., Tao, R., and Xu, J.: China's Sloping Land Conversion  
718 Programme four years on: current situation, pending issues, *International Forestry*  
719 *Review*, 6 (3–4), 317–326, 2004.

720 Yang, H., Wang, G., Yang, Y., Xue, B., and Wu, B.: Assessment of the impacts of land  
721 use changes on nonpoint source pollution inputs upstream of the Three Gorges  
722 Reservoir, *The Scientific World Journal*, 2014, 15 pages, 2014.

723 Yang, J., Reichert, P., Abbaspour, K. C., Xia, J., and Yang, H.: Comparing uncertainty  
724 analysis techniques for a SWAT application to the Chaohe Basin in China, *Journal of*  
725 *Hydrology*, 358, 1–23, 2008.

726 Zhang, S. L., Wang, Y. H., Yu, P. T., Zhang, H. J., and Tu, X. W.: Impact of human  
727 activities on the spatial and temporal variation of runoff of Jinghe Basin, Northwest  
728 China, *Journal of Arid Land Resource and Environment*, 25 (6), 66–72, 2011. (in  
729 Chinese with English abstract)

730 Zhang, X. P., Zhang, L., Zhao, J., Rustomji, P., and Hairsine, P.: Responses of  
731 streamflow to changes in climate and land use/cover in the Loess Plateau, China,  
732 *Water Resources Research*, 44, W00A07.1–W00A07.12, 2008.

733 Zhang, Y., Fu, G., Sun, B., Zhang, S., and Men B.: Simulation and classification of the  
734 impacts of projected climate change on flow regimes in the arid Hexi Corridor of  
735 Northwest China, *Journal of Geophysical Research: Atmospheres*, 120, 7429–7453,  
736 2015.

737 Zhao, A. Z., Zhu, X. F., Liu, X. F., Pan, Y. Z., and Zuo, D. P.: Impacts of land use  
738 change and climate variability on green and blue water resources in the Weihe River  
739 Basin of northwest China, *CATENA*, 137, 318–327, 2016.

740 Zhao, L., Lyu, A. F., Wu, J. J., Hayes, M., Tang, Z. H., He, B., Liu J. H., and Liu, M.:  
741 Impact of meteorological drought on streamflow drought in Jinghe River Basin of  
742 China, *Chinese Geographical Science*, 24 (6), 694–705. doi:  
743 10.1007/s11769-014-0726-x, 2014.

744 Zuo, D. P., Xu, Z. X., Wu, W., Zhao, J., and Zhao, F. F.: Identification of Streamflow

745      Response to Climate Change and Human Activities in the Wei River Basin, China,  
746      Water Resources Management, 28 (3), 833–851, 2014.  
747

748 **Table 1.** Calibrated values of the six parameters in SWAT

No.	Parameter name	Description	Range	Calibrated value
1	CN <sub>2</sub>	SCS runoff curve number for moisture condition II	-8--+8	-8
2	ESCO	Soil evaporation compensation factor	0-1	0.1
3	SQL_AWC	Available water capacity of the soil layer	0-1	0.05
4	CH_K <sub>2</sub>	Channel conductivity	0-150	0.35
5	ALPHA_BF	Baseflow alpha factor	0-1	0.01
6	SURLAG	Surface runoff coefficient	0-10	0.85

749

750

751

**Table 2.** SWAT performance of runoff simulations according to the Nash–Sutcliffe coefficient (Moriassi et al., 2007).

752

Simulation performance	Nash–Sutcliffe coefficient ( <i>Ens</i> )
Very good	$0.75 < Ens \leq 1.00$
Good	$0.65 < Ens \leq 0.75$
Satisfactory	$0.50 < Ens \leq 0.65$
Unsatisfactory	$Ens \leq 0.50$

753

754

755

**Table 3.** Simulated annual runoff by SWAT under different scenarios considering

756

both LULC and climate.

	Scenarios	Climate	LULC	Simulation ( $\text{m}^3 \text{s}^{-1}$ )	Runoff change ( $\text{m}^3 \text{s}^{-1}$ )	Runoff change (%)
	LULC and					
S1	meteorological data from the 1970s	1970s	1970s	84.10	–	–
	Changing LULC while					
S2	holding climate constant	1970s	1980s	86.40	+2.30	+7.73
	Changing climate while					
S3	holding LULC constant	1980s	1970s	110.17	+26.07	+87.63
	LULC and					
S4	meteorological data from the 1980s	1980s	1980s	113.85	+29.75	–
	Changing LULC while					
S5	holding climate constant	1980s	1990s	107.02	-6.83	-54.25
	Changing climate while					
S6	holding LULC constant	1990s	1980s	108.61	-7.04	-55.92
	LULC and					
S7	meteorological data from the 1990s	1990s	1990s	101.26	-12.59	–
	Changing LULC while					
S8	holding climate constant	1990s	2000s	90.20	-11.06	-70.67
	Changing climate while					
S9	holding LULC constant	2000s	1990s	94.67	-6.59	-42.11
	LULC and					
S10	meteorological data from the 2000s	2000s	2000s	85.61	-15.65	–

757

758

**Table 4.** Nash-Sutcliffe coefficient (*Ens*) statistics in the SWAT calibration and validation periods.

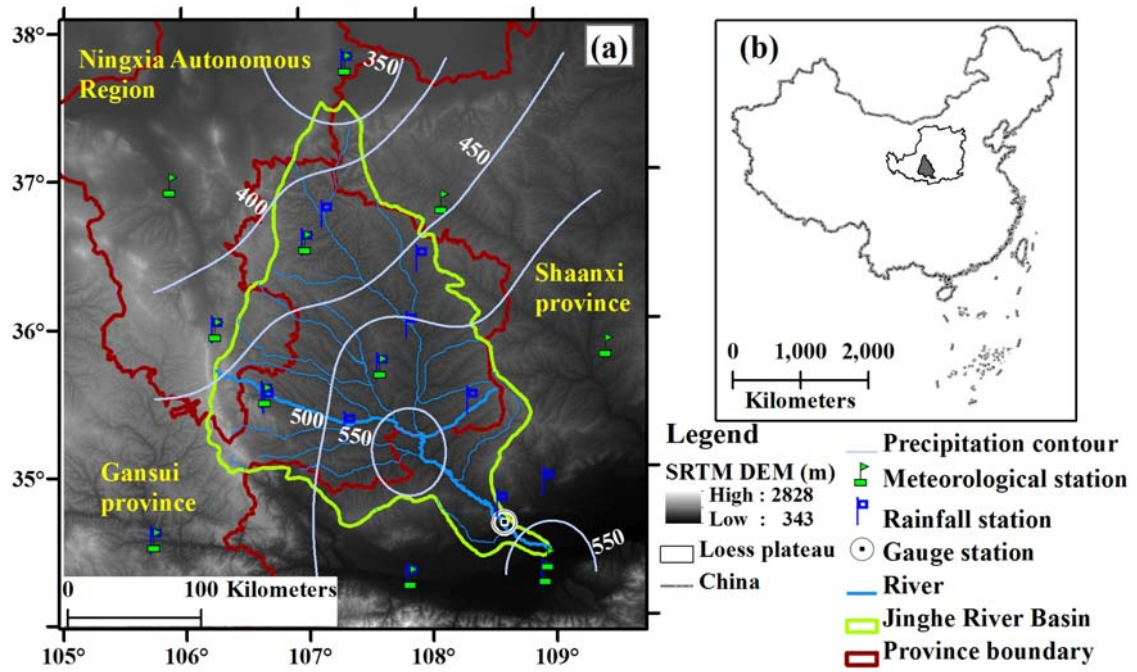
759

Statistic	Calibration from		Validation from	
	1971–1980		1981–1990	
	monthly	yearly	monthly	yearly
<i>N</i>	120	10	120	10
Minimum	0.58	0.53	0.54	0.58
Maximum	0.95	0.98	0.81	0.9
Mean	0.72	0.76	0.69	0.73

760

761





762

763

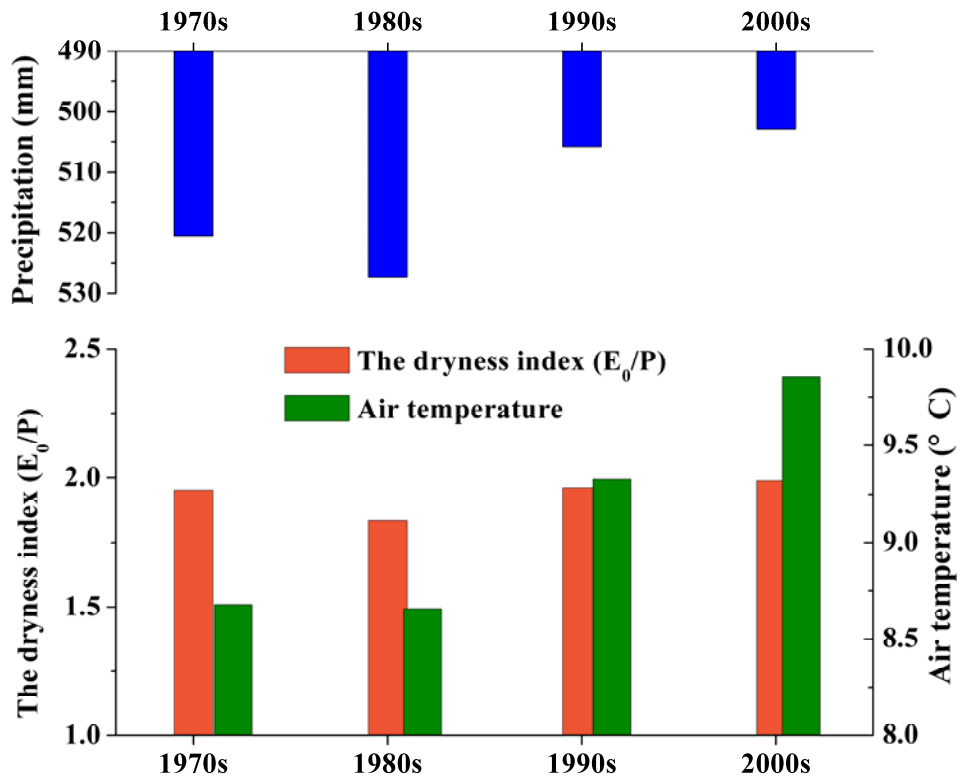
764

765

766

767

**Figure 1.** Geographic information regarding the study area: (a) Location and SRTM DEM of the Jinghe River Basin and (b) schematic of the selected study area in China. Precipitation (mm) is averaged and interpolated from meteorological data between 1970 and 2010.



768

769

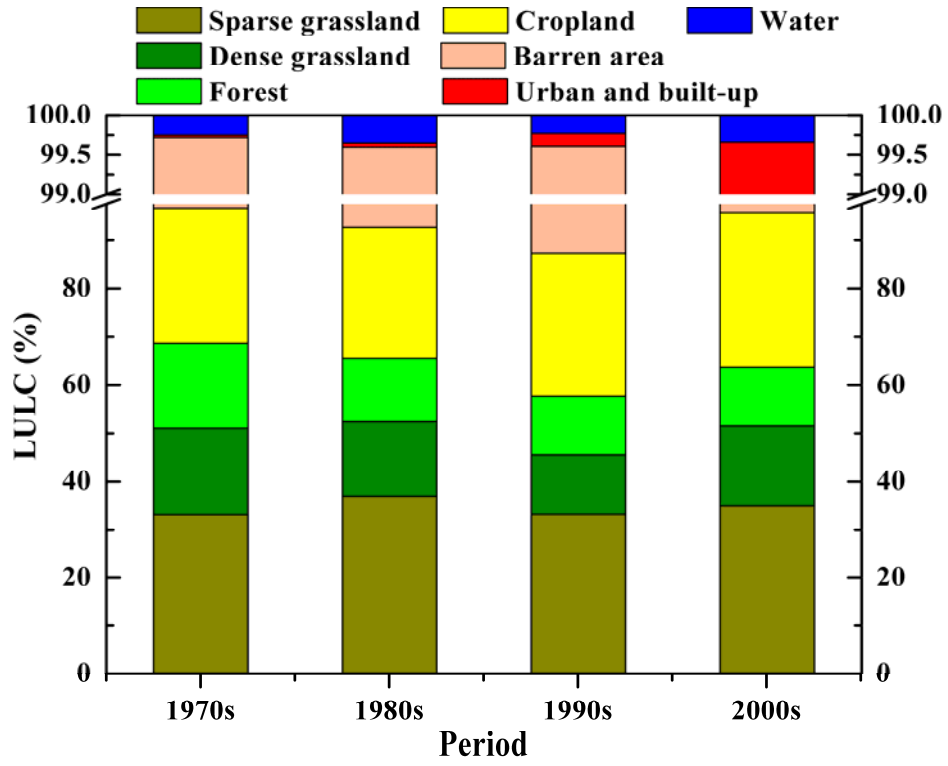
770

771

772

773

**Figure 2.** Variation in decadal mean precipitation (top), dryness index, and air temperature (bottom) in the Jinghe River Basin from the 1970s to the 2000s. The dryness index was defined as the ratio of annual potential evapotranspiration ( $E_0$ ) to annual precipitation ( $P$ ).



774

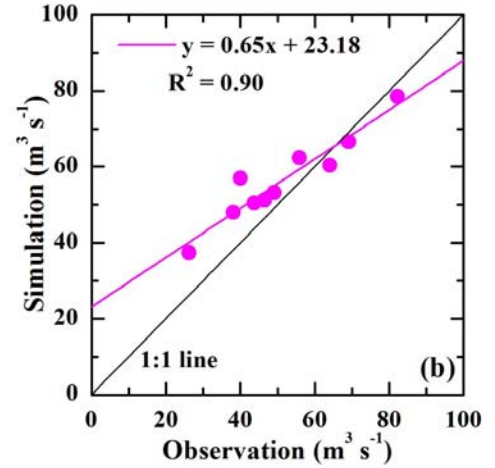
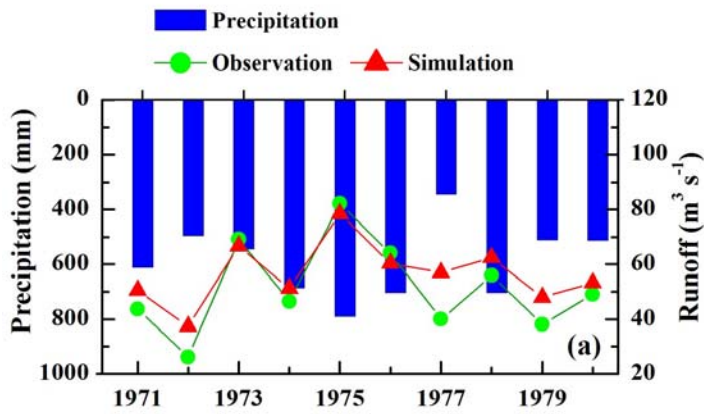
775

**Figure 3.** LULC composition and its change in the Jinghe River Basin from the 1970s

776

to the 2000s.

777



778

779

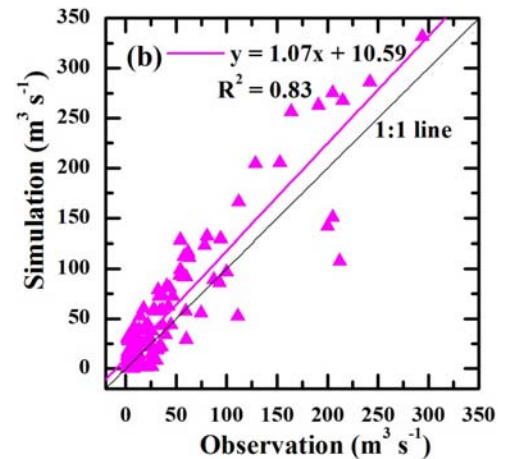
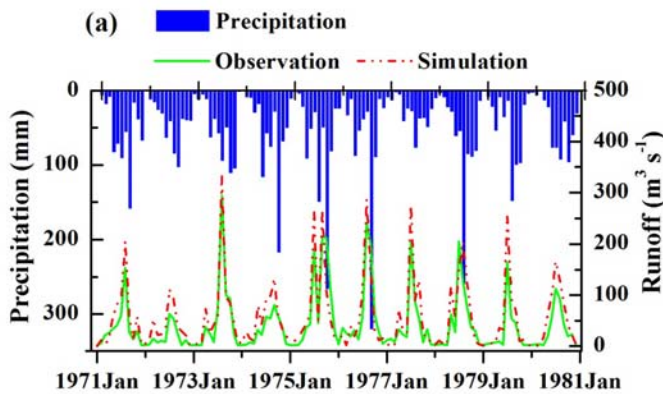
780

781

782

783

**Figure 4.** Comparison of observed and simulated runoff at the yearly scale in the Jinghe River Basin during the calibration period from 1971 to 1980. Fig. 4(b) is redrawn from Qiu et al. (2011).



784

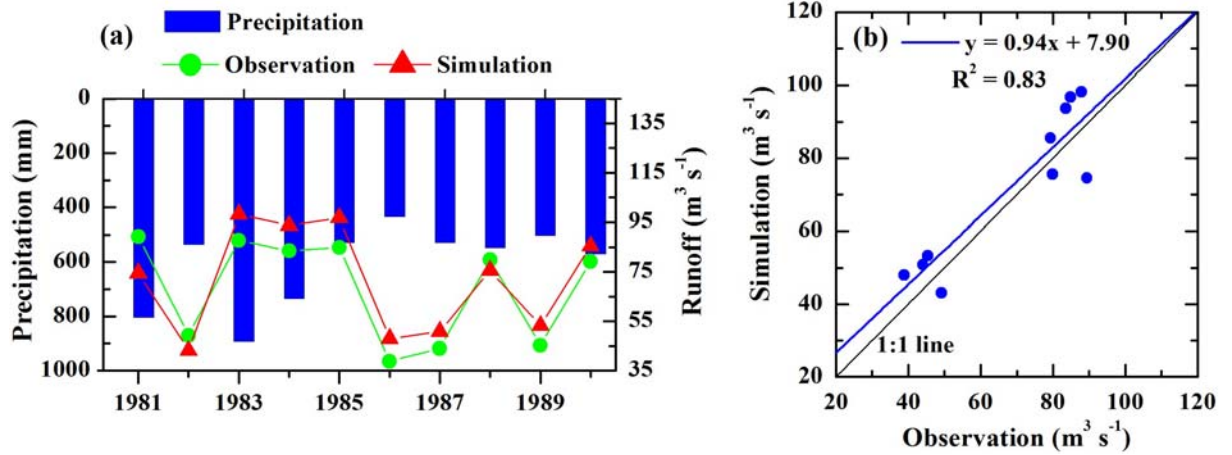
785

786

787

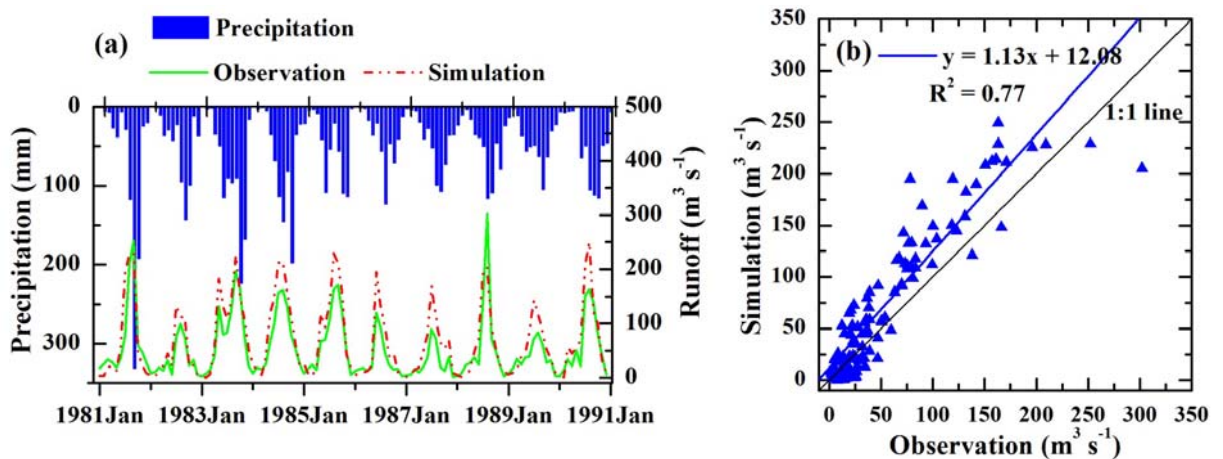
788

**Figure 5.** Comparison of observed and simulated runoff at the monthly scale in the Jinghe River Basin during the calibration period from 1971 to 1980. Fig. 5(b) is redrawn from Qiu et al. (2011).



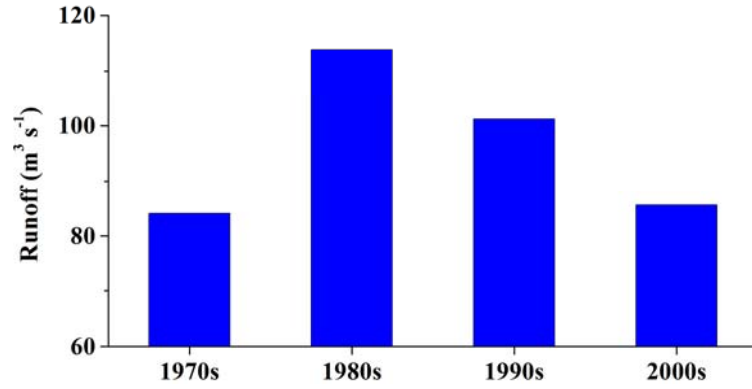
789  
790  
791  
792  
793  
794

**Figure 6.** Comparison of observed and simulated runoff at the yearly scale in the Jinghe River Basin during the validation from 1981 to 1990. Fig. 6(b) is redrawn from Qiu et al. (2011).



795  
796  
797  
798  
799

**Figure 7.** Comparison of observed and simulated runoff at the monthly scale in the Jinghe River Basin during the validation period from 1981 to 1990. Fig. 7(b) is redrawn from Qiu et al. (2011).



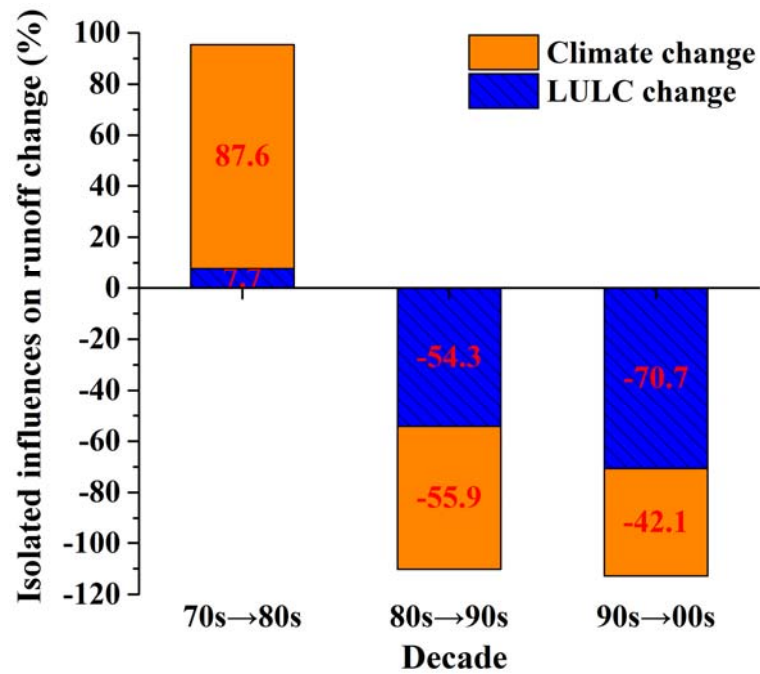
800

801

**Figure 8.** Variation in mean annual surface runoff at the decadal scale in the Jinghe River Basin from the 1970s to the 2000s.

802

803



804

805

**Figure 9.** Isolated impacts of LULC and climate changes on surface runoff. Positive values indicate that runoff increased due to these factors, whereas negative values

806

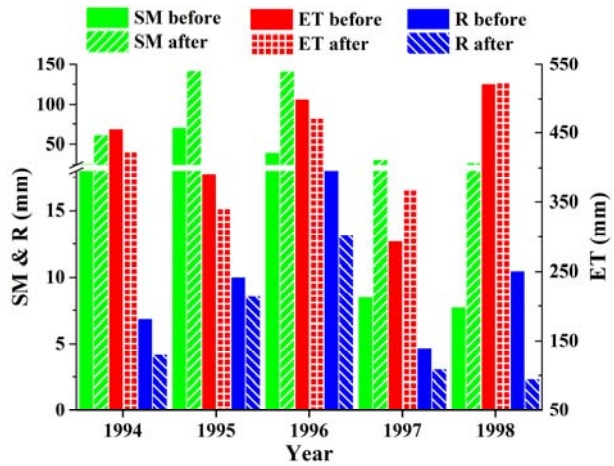
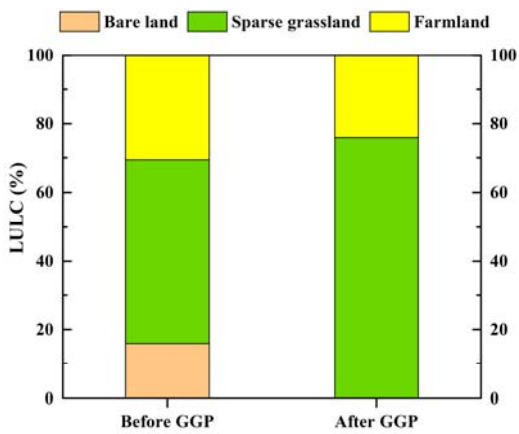
807

indicate that runoff decreased due to these factors. The summation of the isolated

808

influences is not equal to 100% due to simulation uncertainty (see section 4.2 for details).

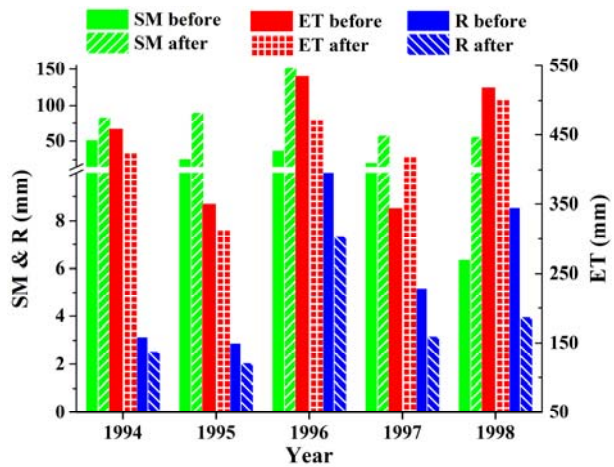
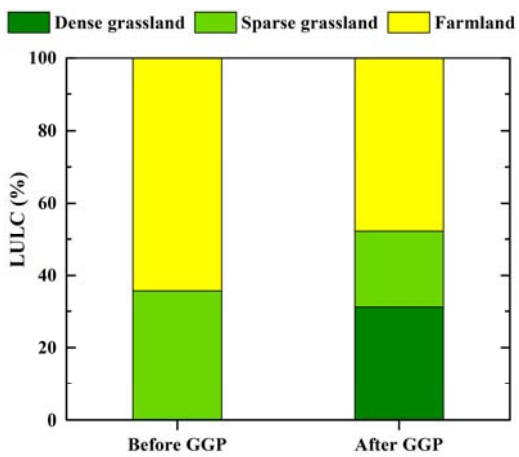




809

810

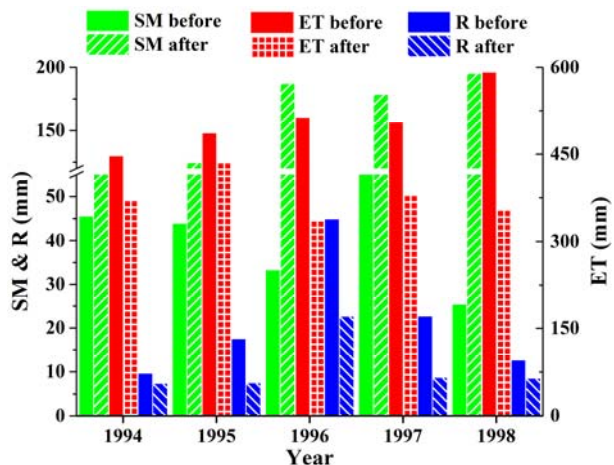
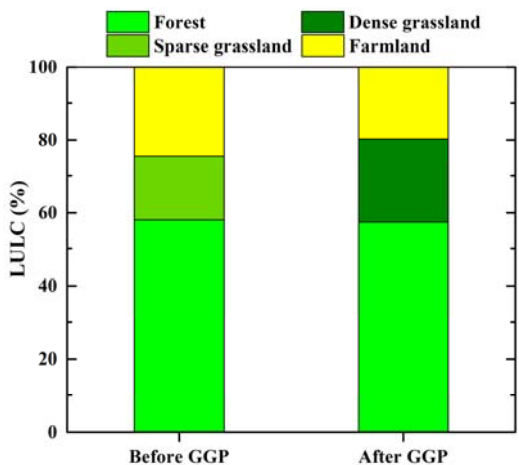
(a) upstream



811

812

(b) midstream



813

814

(c) downstream

815

816

817

818

**Figure 10.** Impact of LULC changes on surface runoff in selected sub-basins distributed in the upstream, midstream, and downstream areas of the basin. The left column shows the land use types and corresponding ratios, and the right column shows the simulated changes of the soil moisture content (SM), evapotranspiration (ET), and

819 surface runoff (R) before and after the Grain for Green Program (GGP) scenarios while  
820 holding climate constant.